EFFECT OF TEMPERATURE ON THE PERFORMANCE OF A CYLINDRICAL MICROSTRIP PRINTED ANTENNA FOR TM_{01} MODE USING DIFFERENT SUBSTRATES

A. Elrashidi *, K. Elleithy * and Hassan Bajwa†
*Department of Computer and Electrical Engineering
† Department of Electrical Engineering
University of Bridgeport, 221 University Ave,
Bridgeport, CT, USA
aelrashi@Bridgeport.edu

ABSTRACT

A temperature is one of the parameters that have a great effect on the performance of microstrip antennas for TM01 mode. The effect of temperature on a resonance frequency, input impedance, voltage standing wave ratio, and return loss on the performance of a cylindrical microstrip printed antenna is studied in this paper. The effect of temperature on electric and magnetic fields are also studied. Three different substrate materials RT/duroid-5880 PTFE, K-6098 Teflon/Glass, and Epsilam-10 ceramic-filled Teflon are used for verifying the new model for a microstrip antenna for its flexibility on cylindrical bodies.

KEYWORDS
Temperature, Voltage Standing Wave Ratio VSWR, Return loss S11, effective dielectric constant, Transverse Magnetic TM01 model.

1. INTRODUCTION

Due to unprinted growth in wireless applications and increasing demand of low cost solutions for RF and microwave communication systems, the microstrip flat antenna, has undergone tremendous growth recently. Though the models to analyze microstrip structures have been widely accepted, effect of curvature on dielectric constant and antenna performance has not been studied in detail. Low profile, low weight, low cost and its ability of conforming to curve surfaces [1], conformal microstrip structures have also witnessed enormous growth in the past few years. Applications of microstrip structures include Unmanned Aerial Vehicle (UAV), planes, rocket, radars and communication industry [2]. Some advantages of conformal antennas over the planer microstrip structure include, easy installation (randome not needed), capability of embedded structure within composite aerodynamic surfaces, better angular coverage and controlled gain, depending upon shape [3, 4]. While Conformal Antenna provide potential solution for many applications it has some drawbacks due to bedding [5], those drawbacks include phase, impedance, and resonance frequency errors due to the stretching and compression of the dielectric material along the inner and outer surfaces of conformal surface. Changes in the dielectric constant and material thickness also affect the performance of the antenna. Analysis tools for conformal arrays are not mature and fully developed [6]. Dielectric

DOI : 10.5121/ijcnc.2011.3501

materials suffer from cracking due to bending and that will affect the performance of the conformal microstrip antenna.

In some applications, a microstrip antenna is required to operate in an environment that is close to what is defined as room or standard conditions [7]-[11]. However, antennas often have to work in harsh environments characterized by large temperature variations [12]. In this case, the substrate properties suffer from some variations. The effect of that variation on the overall performance of a microstrip conformal antenna is very important to study under a wide range of temperature.

2. BACKGROUND

Conventional microstrip antenna has a metallic patch printed on a thin, grounded dielectric substrate. Although patch can be of any shape rectangular patches, as shown in Figure 1 [13], are preferred due to easy calculation and modeling.

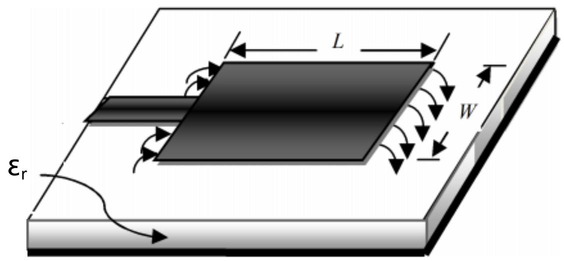

Figure. 1. Rectangular microstrip antenna

Fringing field has a great effect on the performance of a microstrip antenna. In microstrip antennas the electric field in the center of the patch is zero. The radiation is due to the fringing field between the periphery of the patch and the ground plane. For rectangular patch shown in the Figure 2, there is no field variation along the width and thickness. The amount of fringing field is a function of the dimensions of the patch and the height of the substrate. Higher the substrate the more is the fringe fields.

Due to effect of fringing a microstrip patch antenna would look electrically wider compared to its physical dimensions. As shown in Figure 2, waves travel both in substrate and air. Thus an effective dielectric constant ε_{reff} is to be introduced. The effective dielectric constant ε_{reff} take in account both the fringing and the wave propagation in the line.

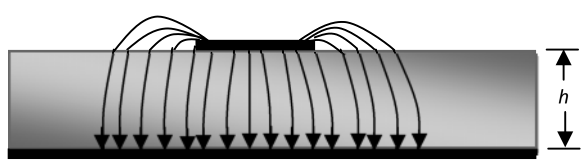

Figure 2. electric field lines (Side View).

The expression for the effective dielectric constant is introduced by A. Balanis [13], as shown in Equation 1.

$$\varepsilon_{reff} = \frac{\varepsilon_r + 1}{2} + \frac{\varepsilon_r - 1}{2}\left[1 + 12\frac{h}{w}\right]^{-\frac{1}{2}} \quad (1)$$

The length of the patch is extended on each end by *ΔL* is a function of effective dielectric constant ε_{reff} and the width to height ratio (*W/h*). *ΔL* can be calculated according to a practical approximate relation for the normalized extension of the length [14], as in Equation 2.

$$\frac{\Delta L}{h} = 0.412 \frac{(\varepsilon_{reff} + 0.3)\left(\frac{W}{h} + 0.264\right)}{(\varepsilon_{reff} - 0.258)\left(\frac{W}{h} + 0.8\right)} \qquad (2)$$

The effective length of the patch is L_{eff} and can be calculated as in Equation 3.

$$L_{eff} = L + 2\Delta L \qquad (3)$$

By using the effective dielectric constant (Equation 1) and effective length (Equation 3), we can calculate the resonance frequency of the antenna f_r and all the microstrip antenna parameters.

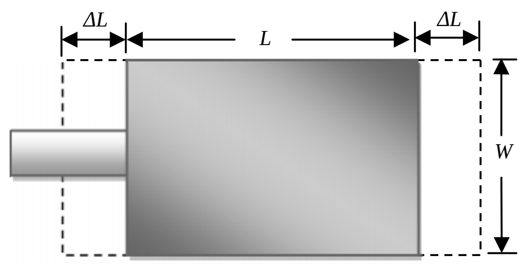

Figure. 3. Physical and effective lengths of rectangular microstrip patch.

Cylindrical-Rectangular Patch Antenna

All the previous work for a conformal rectangular microstrip antenna assumed that, the curvature does not affect the effective dielectric constant and the extension on the length. Effect of curvature on the resonant frequency has been presented previously [15]. In this paper we present the effect of fringing field on the performance of a conformal patch antenna. A mathematical model that includes the effect of curvature on fringing filed and on antenna performance is presented. The cylindrical-rectangular patch is the most famous and popular conformal antenna. The manufacturing of this antenna is easy with respect to spherical and conical antennas.

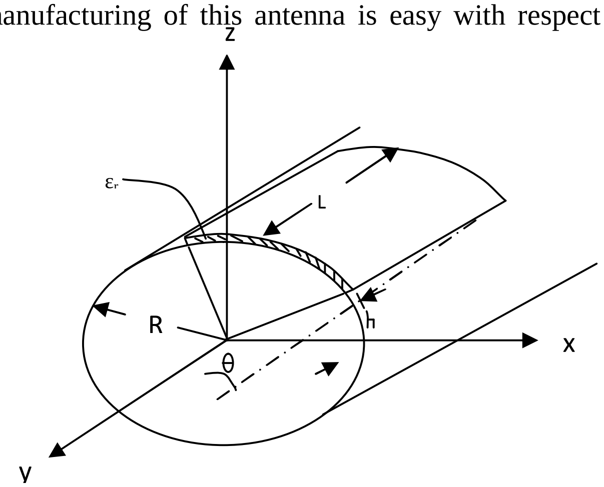

Figurer 4: Geometry of cylindrical-rectangular patch antenna

Effect of curvature of conformal antenna on resonant frequency been presented by Clifford M. Krowne [15] as:

$$(f_r)_{mn} = \frac{1}{2\sqrt{\mu\varepsilon}}\sqrt{\left(\frac{m}{2\theta a}\right)^2 + \left(\frac{n}{2b}\right)^2} \quad (4)$$

Where *2b* is a length of the patch antenna, *a* is a radius of the cylinder, *2θ* is the angle bounded the width of the patch, *ε* represents electric permittivity and *μ* is the magnetic permeability as shown in Figure 4.

3. TEFLON AS A SUBSTRATE IN MICROSTRIP PRINTED ANTENNAS

T. Seki et.al. introduced a highly efficient multilayer parasitic microstrip antenna array that is constructed on a multilayer Teflon substrate for millimeter-wave system [16]. This antenna achieves a radiation efficiency of greater than 91% and an associated antenna gain 11.1 dBi at 60 GHz. The antenna size is only 10 mm × 10 mm. So, using Teflon as a substrate material in microstrip antennas is highly recommended nowadays, especially in conformal microstrip antennas for its ability to bend over any surface [17].

4. EFFECT OF TEMPERATURE ON A TEFLON SUBSTRATE

P. Kabacik et.al. studied the effect of temperature on substrate parameters and their effect on microstrip antenna performance [18]. Dielectric constant and dispersion factor are plotted as a function of temperature for a wide temperature ranges equivalent to those in airborne applications. The authors used Teflon-glass and ceramic-Teflon materials as a substrate for microstrip antenna. Also, the authors conclude that, the measured dielectric constant value was greater than the one specified in the data sheets.

The effect of temperature on Teflon material on the electrical properties is studied by A. Hammoud et.al. [19]. In this work, the authors indicated that the dielectric properties of Teflon is temperature dependence as illustrated in the next chapter.
The effect of high temperature on a Teflon substrate material on electrical properties, dielectric constant, mechanical properties, and thermal properties are also studied [20] - [23].

5. TEMPERATURE EFFECT ON THE ANTENNA PERFORMANCE

For a microstrip antenna fixed on a projectile that fly at a long distance, the temperature will be an issue for the performance of that antenna. A large variation of temperature (-25 ^{0}C, 25 ^{0}C and 75 ^{0}C) will be considered during the studying. The effect of the temperature on the substrate material of the microstrip antenna is studied in this paper [24].

The Temperature affects the dielectric constant of the substrate and also affects expansion of the material which increase or decrease the volume of the dielectric with increasing or decreasing the temperature [25]. The recorded dielectric constant of the Teflon at low frequencies is 2.07 at room temperature but due to the dependency of the dielectric constant on the operating frequency [26], the dielectric constant decreases to be around 2.02 at the range of Giga hertz.

The measured relationship between temperature and dielectric constant is given in [26] as shown in the Figure 3 as an actual data, and the fitted data that we already did using MATLAB software, as a linear relation, is also shown bellow.

The linear Equation for that relation is illustrated in the following Equation:

$$\varepsilon_r = 0.00072\,T + \varepsilon_{r(T=27\,℃)} \tag{5}$$

Linear thermal expansion can be calculated as in the following formula [25]:

$$\Delta L_{thermal} = L \times \alpha \times \Delta T \tag{6}$$

where: $\Delta L_{\text{thermal}}$ is the expansion in length.
L is the original length at certain temperature.
α is the coefficient of thermal expansion.
ΔT is the difference of temperature.

So, the linear thermal expansion which is represents the ratio between $\Delta L_{\text{thermal}}$ and L is given by [26], which is shown in Figure 4. The actual and fitted curves and the fitted Equation are given bellow:

$$\frac{\Delta L_{thermal}}{L} = 7.2 \times 10^{-8} T^3 + 3.5 \times 10^{-8} T^2 + 0.013\,T - 0.26 \tag{7}$$

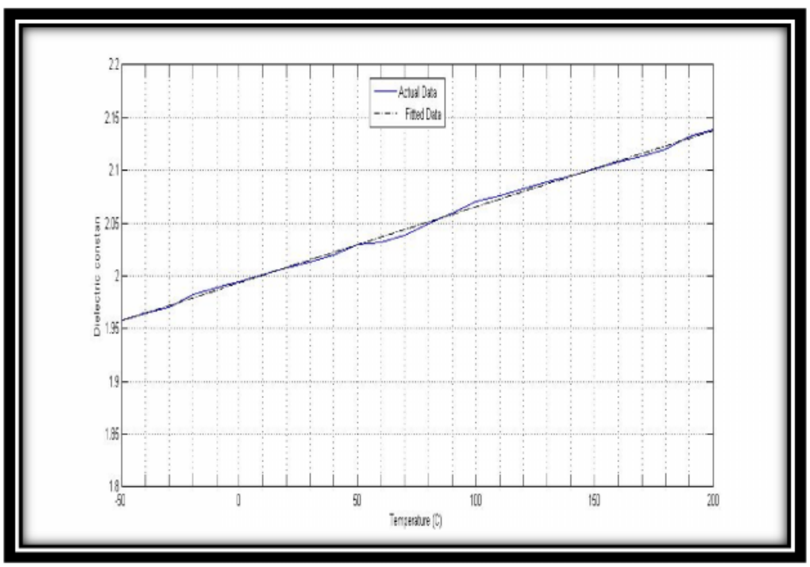

Figure 3. Dielectric constant vs. temperature for Teflon substrate at the range of GHz.

Hence, we can calculate the effect of temperature on the expansion of the dimensions of the substrate and on the dielectric constant of the microstrip antenna. The new length or width of the microstrip antenna will be due to the effect of fringing field and thermal expansion, so the new length or width will take the form of Equation (8):

$$L = L_0 + \Delta L_{frining} + \Delta L_{thermal} \tag{8}$$

Also, the effect of fringing field and temperature on the dielectric constant of the substrate will be considered in the calculations of antenna parameters.

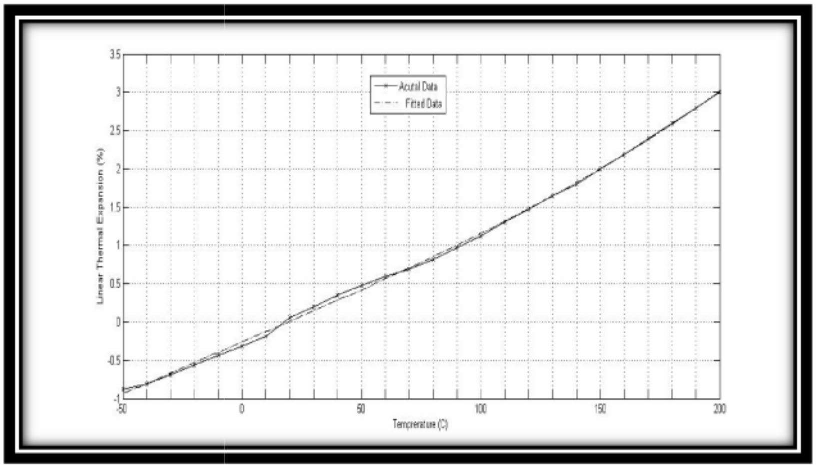

Figure 4. Linear thermal expansion vs. temperature for Teflon substrate.

2. Results

For a range of GHz, the dominant mode is TM_{01} for $h<<W$ which is the case. Also, for the antenna operates at the range of 2.4 GHz we can get the following dimensions; the original length is 41.5 mm, the width is 50 mm, substrate height is 0.8 mm and for different lossy substrate we can get the effect of curvature on the effective dielectric constant and the resonance frequency.

Three different substrate materials RT/duroid-5880 PTFE, K-6098 Teflon/Glass, and Epsilam-10 ceramic-filled Teflon are used for verifying the new algorithm. The dielectric constants for the used materials are 2.07, 2.5 and 10 respectively with a tangent loss 0.0015, 0.002 and 0.0004 respectively.

The relation between the effective dielectric constant and radius of curvature for different values of temperature, -25, 25 and 75 ^{0}C is shown in Figure 7.

The relation between curvature and effective dielectric constant was introduced in [27], and by using the generated model we can caudate the input impedance, VSWR and return loss.

a) RT/duroid-5880 PTFE substrate

Resonance frequency for TM_{01} as a function of curvature with different values of temperatures is introduced in Figure 8. The resonance frequency decreases with increasing temperature because of inverse relation between effective dielectric constant and temperature. Due to temperature, decreasing in resonance frequency for every 50 ^{0}C in temperature is almost 20 MHz.

Real part of input impedance at 50 mm radius of curvature at different values of temperatures is illustrated in Figure 9. As notice from the previous Figures, the resonance frequency decreases with increasing temperature by 20 MHz for every 50 ^{0}C. The same thing is also noted from Figure 9, for every 50 ^{0}C increasing in temperature, the resonance frequency is decreasing by almost 20 MHz. The peak value is also increasing with increasing temperature by very small values.

Figure 10 shows the effect of temperature on the imaginary part of input impedance which gives the same results as a real part. Reactance equal to zero at the same value of frequency of a peak value for a real part of input impedance, this frequency is called a resonance frequency.

VSWR and Return loss are shown in Figures 11 and 12 respectively for 50 mm radius of curvature and temperatures -50, 27 and 75 ^{0}C. We can easily notice that, decreasing in temperature by 50 ^{0}C leads to increasing in frequency for minimum values of VSWR and return loss by 20 MHz. VSWR values are between 1 and 2 at the resonance frequencies also, return losses are between -23 and -24 dB which is very efficient in the antenna manufacture process and gives a good performance.

Normalized electric and magnetic fields as a function of temperature at 50 mm radius of curvature and for different values of temperatures, -25, 27, 75 and 150 ^{0}C, are shown bellow in Figures 13 and 14 respectively. The effect of temperature for a wide range, from -25 to 150 ^{0}C, in the electric field at the same value of frequency shows the effect of temperature is in the range of 10% of the value. The same results are obtained in the normalized magnetic field values as a function of temperature.

Hence, we can note that, the effect of temperature on radiation patterns is less than the effect of curvature. So, the radiation pattern angle is almost the same and field strength is slightly different in a range of 200 ^{0}C.

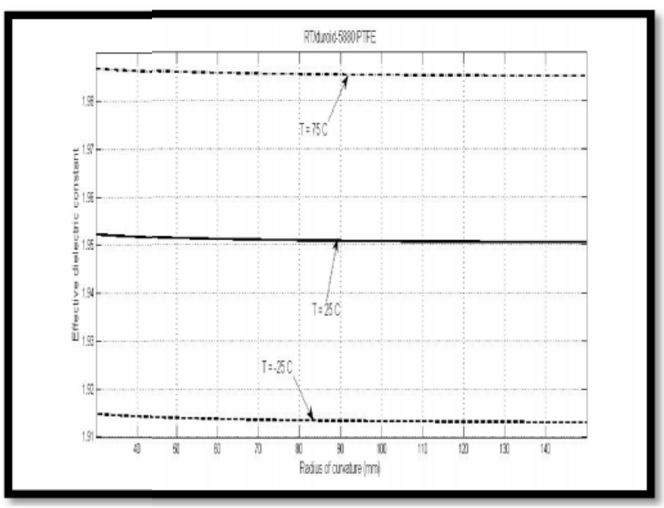

Figure. 7. Effective dielectric constant versus radius of curvature for cylindrical-rectangular and a flat microstrip printed antenna at different temperatures 75, 25 and -25 ^{0}C.

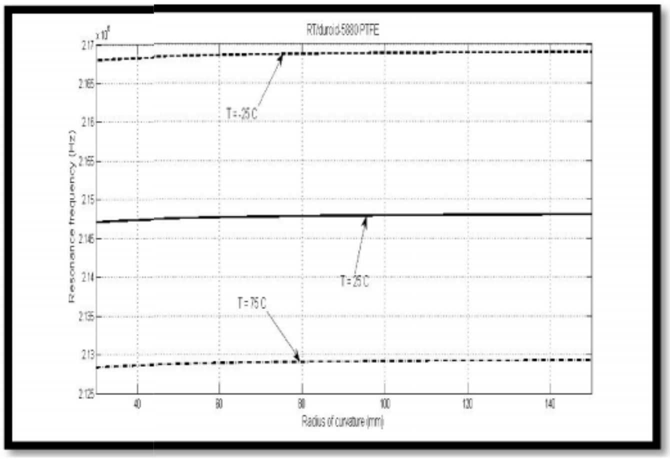

Figure. 8. Resonance frequency versus radius of curvature for cylindrical-rectangular and a flat microstrip printed antenna at different temperatures 75, 25 and -25 ^{0}C.

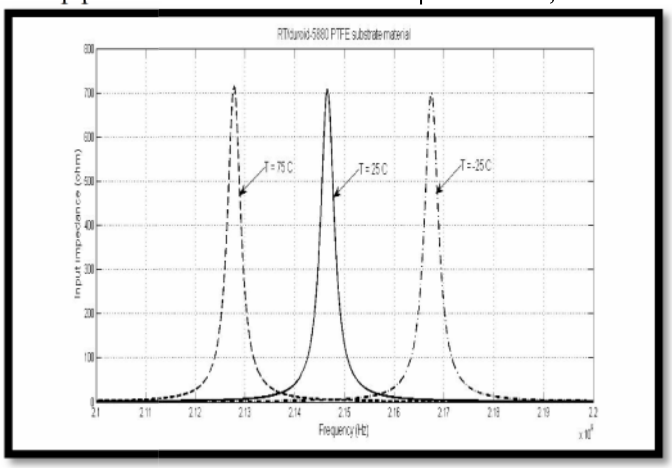

Figure. 9. Real part of the input impedance as a function of frequency at different temperatures 75, 27 and -25 ^{0}C and radius of curvature 50 mm.

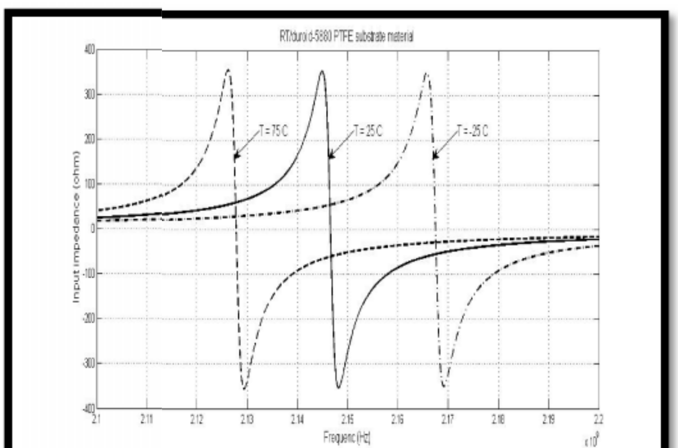

Figure. 10. Imaginary part of the input impedance as a function of frequency at different temperatures 75, 25 and -25 ^{0}C and radius of curvature 50 mm.

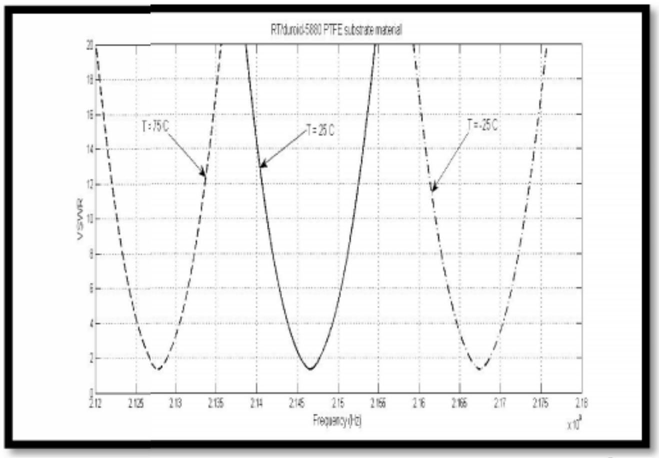

Figure. 11. VSWR versus frequency at different temperatures 75, 25 and -25 ^{0}C and radius of curvature 50 mm.

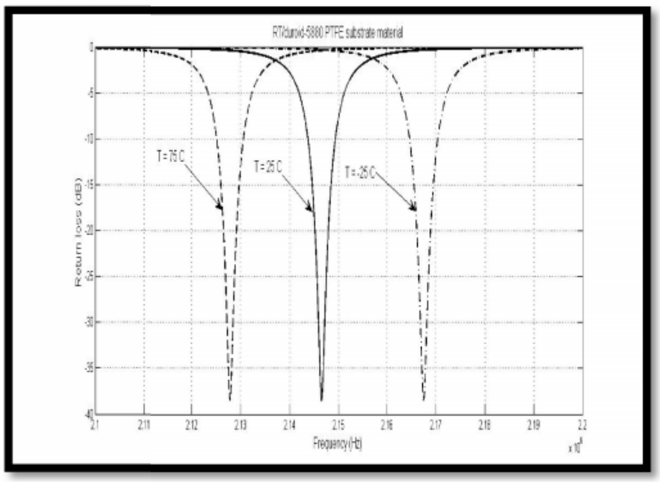

Figure. 12. Return loss (S11) as a function of frequency at different temperatures 75, 25 and -25 ^{0}C and radius of curvature 50 mm.

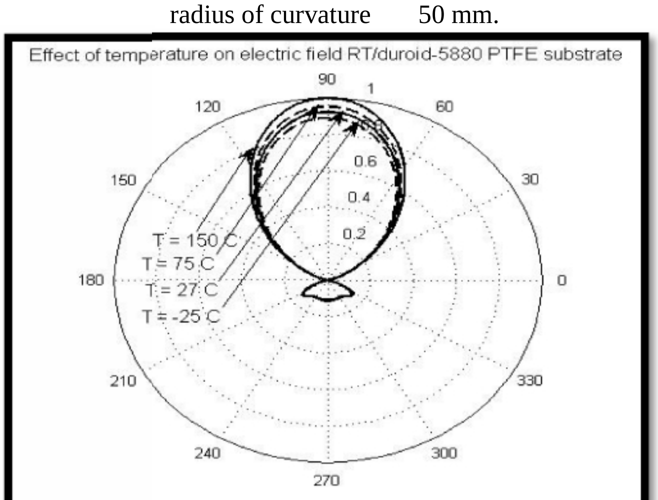

Figure. 13. Normalized electric field for different temperatures 150, 75, 27 and -25 ^{0}C. at $\theta=0:2\pi$ and $\varphi=0^0$ and radius of curvature 50 mm.

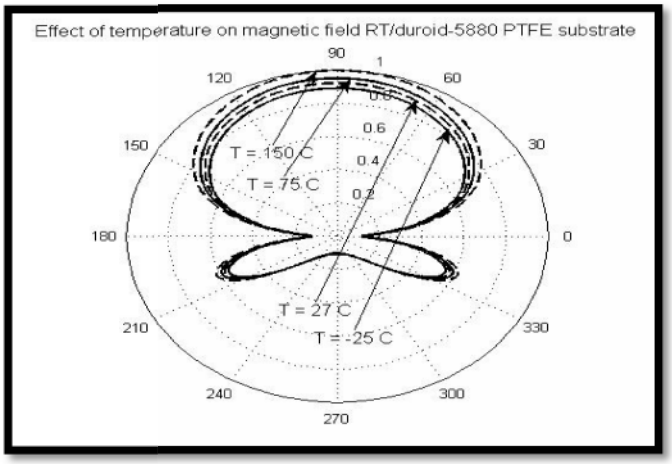

Figure. 14. Normalized magnetic field for different temperatures 150, 75, 27 and -25 ^{0}C. at θ=0:2π and φ=0^0 and radius of curvature 50 mm.

b) *K-6098 Teflon/Glass substrate*

Effect of temperature on a performance of K-6098 Teflon/Glass material is studied in this section. The effect of temperature on the effective dielectric constant is shown in Figure 15. Using Figure 15, we can note that, increasing in temperature leads to increasing in the value of effective dielectric constant by 0.0007 for each Celsius degree.

Effective dielectric constant increases with increasing the temperature due to two reasons:

1. Increasing temperature leads to increasing the collision between atoms and electrons inside the material and hence the speed of light inside the material will decrease which leads to increases the effective dielectric constant.
2. Increasing temperature expands the dielectric material and hence, the distance which electric field goes inside the substrate increases which means, the effective dielectric constant increases.

Resonance frequency for mode TM_{01} as a function of curvature for different values of temperatures is shown in Figure 16; resonance frequency decreases with increasing in temperature, almost 15 MHz decreasing in resonance frequency for 50 ^{0}C increasing in temperature.

Peak values of a real part of input impedance are shifted to the left as shown in Figures 17 and 18 respectively, decreasing in frequency, with increasing in temperature. The difference between peaks of real part of input impedance is almost 15 MHz due to change in temperature by 50 ^{0}C. The same scenario occurred in case of reactance, imaginary part of input impedance, increasing temperature leads to shifting in imaginary part to left.

VSWR and return loss are shown in Figures 19 and 20 respectively. 15 MHz between resonance frequencies for three different temperatures are simply notice in these Figures.

The effect of temperature on normalized electric and magnetic fields are given in Figures 21 and 22 respectively for a wide range of temperatures, -25, 27, 75 and 150 ^{0}C, and for angle θ from 0 to 2π and φ equal to zero. The effect of temperature for a wide range is not very big; it is in a very small range from 90% to 100%.

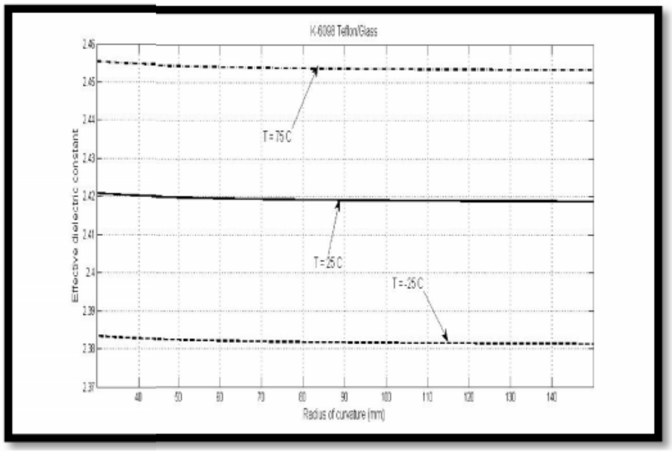

Figure. 15. Effective dielectric constant versus radius of curvature for cylindrical-rectangular and flat microstrip printed antenna at different temperatures 75, 25 and -25 ^{0}C.

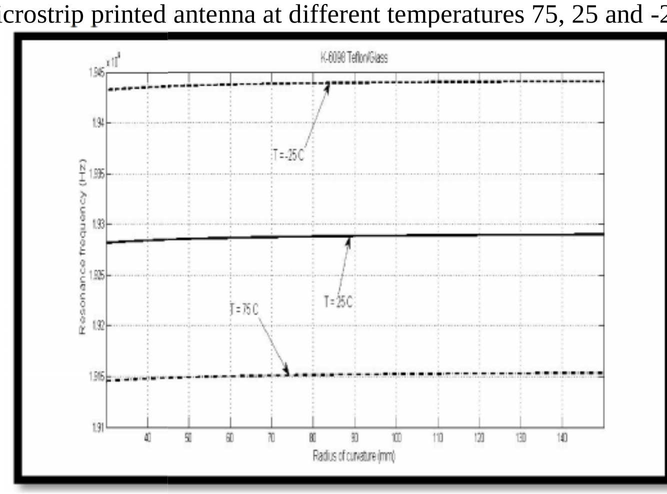

Figure. 16. Resonance frequency versus radius of curvature for cylindrical-rectangular and flat microstrip printed antenna at different temperatures 75, 25 and -25 ^{0}C.

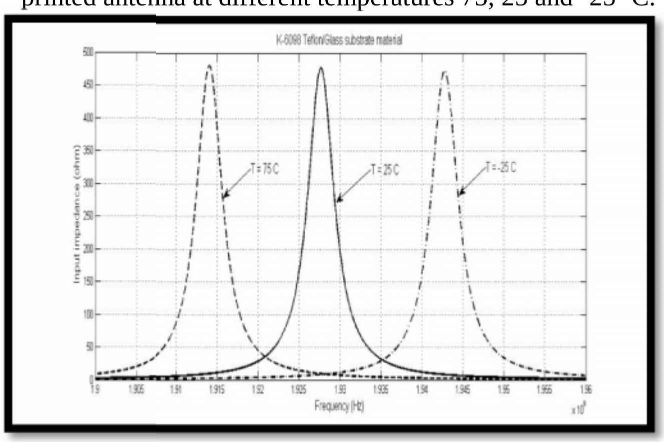

Figure. 17. Real part of the input impedance as a function of frequency at different temperatures 75, 25 and -25 ^{0}C and radius of curvature 50 mm.

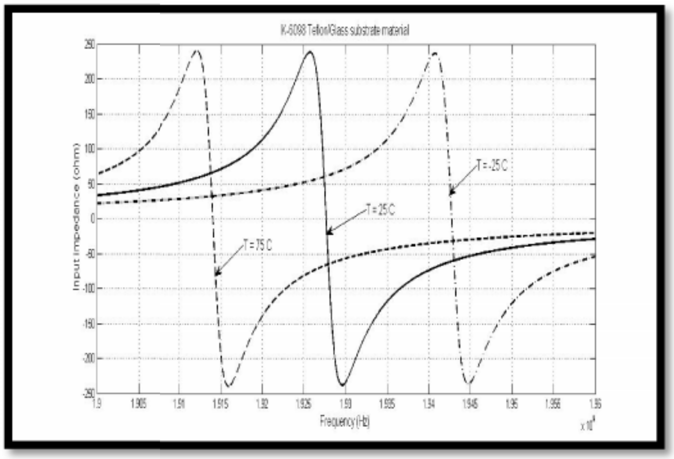

Figure. 18. Imaginary part of the input impedance as a function of frequency at different temperatures 75, 25 and -25 ^{0}C and radius of curvature 50 mm.

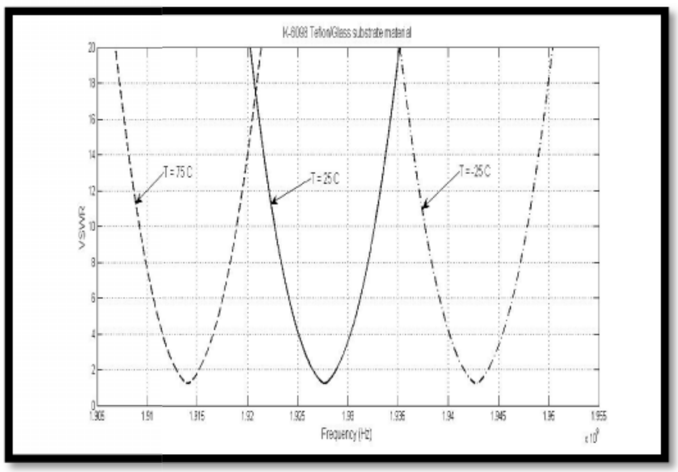

Figure. 19. VSWR versus frequency at different temperatures 75, 25 and -25 ^{0}C and radius of curvature 50 mm.

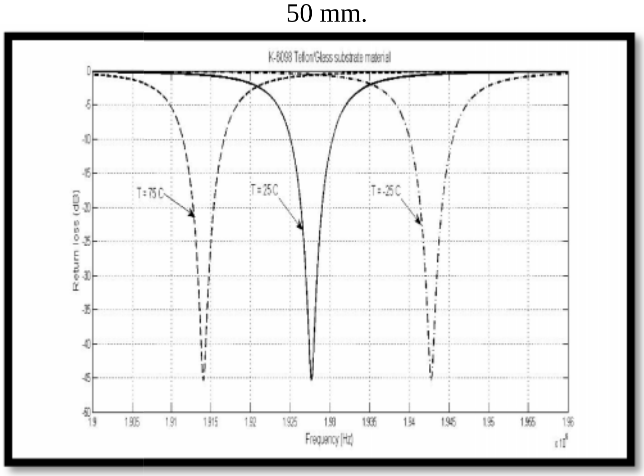

Figure. 20. Return loss (S11) as a function of frequency at different temperatures 75, 25 and -25 ^{0}C and radius of curvature 50 mm.

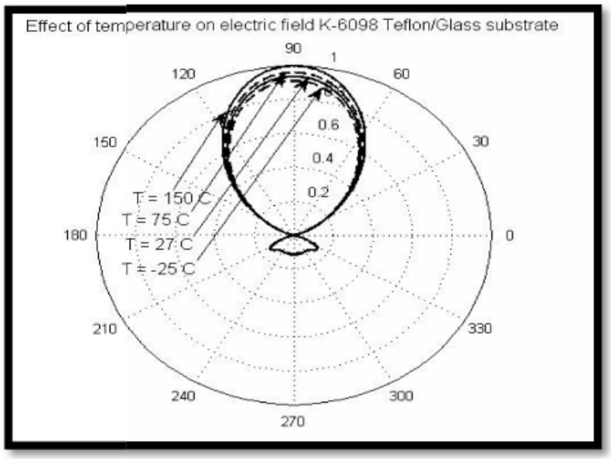

Figure. 21. Normalized electric field for different temperatures 150, 75, 27 and -25 ^{0}C. at θ=0:2π and $\varphi=0^0$ and radius of curvature 50 mm.

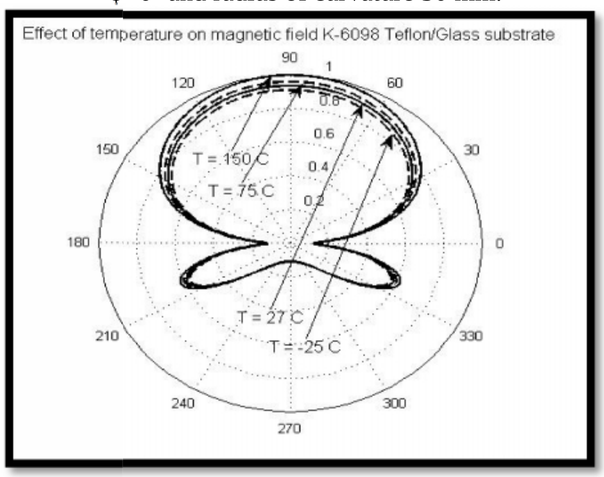

Figure. 22. Normalized magnetic field for different temperatures 150, 75, 27 and -25 ^{0}C. at θ=0:2π and $\varphi=0^0$ and radius of curvature 50 mm.

c) Epsilam-10 ceramic-filled Teflon substrate

For Epsilam-10 ceramic-filled Teflon substrate; the same parameters are also studied in this section. Due to temperature, the effective dielectric constant increases by 0.00068 for increasing temperature by one Celsius degree as shown in Figure 23. This value is less than the other two substrates, which is 0.0007 for K-6098 Teflon/Glass and 0.00074 for RT/duroid-5880 PTFE substrate. Hence; we can conclude that, as the dielectric constant increases, the effect of temperature on the effective value of dielectric constant decreases.

Figure 24 shows the resonance frequency as a function of curvature for different temperatures. The difference between resonance frequencies due to increasing in temperature by 50 ^{0}C is almost 18 MHz.

The real part of input impedance is shown in Figure 25, the resonance value, resistance, of input impedance at temperature 75 ^{0}C is 0.959 GHz and 0.9608 GHz at temperature 27 ^{0}C which means, the difference is 18 MHz.

Imaginary part of input impedance is illustrated in Figure 26 for radius of curvature 50 mm and three values of temperatures -25, 27 and 75 ^{0}C. Resonance values are the same as in real part, peaks of real parts are at the same frequency of zeros for imaginary parts.

VSWR and return loss are shown in Figures 27 and 28 respectively, minimum values of VSWR and return loss are in the same frequency for a peak values real part of input impedance and same values of imaginary parts that give a zeros. Return loss value is almost -16 dB for all values of temperatures.

Effect of temperature on normalized electric and magnetic fields are given in Figures 29 and 30 respectively. The effect of temperature on electric and magnetic fields is very small and we could not determine the difference between curves. So, we can conclude that, the temperature has no major effect on the radiation pattern on Epsilam-10 ceramic-filled Teflon substrate for dielectric constant 10 and tangent loss 0.0015.

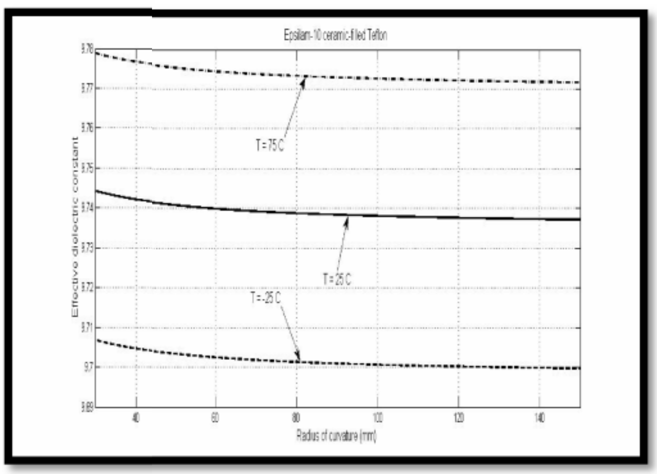

Figure. 23. Effective dielectric constant versus radius of curvature for cylindrical-rectangular and flat microstrip printed antenna at different temperatures 75, 25 and -25 ^{0}C.

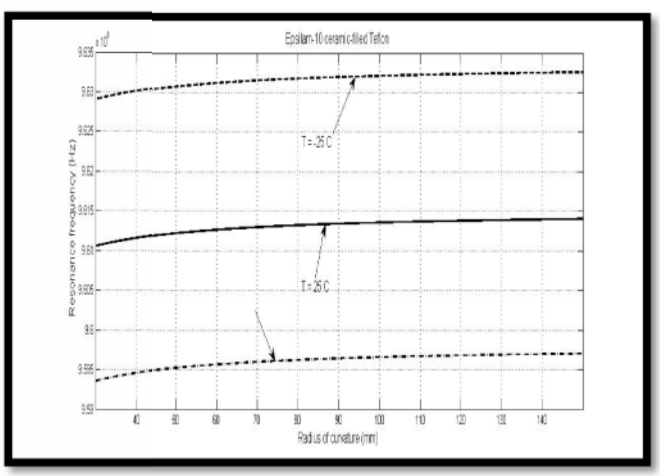

Figure. 24. Resonance frequency versus radius of curvature for cylindrical-rectangular and flat microstrip antenna for TM_{01} at different temperatures 75, 25 and -25 ^{0}C.

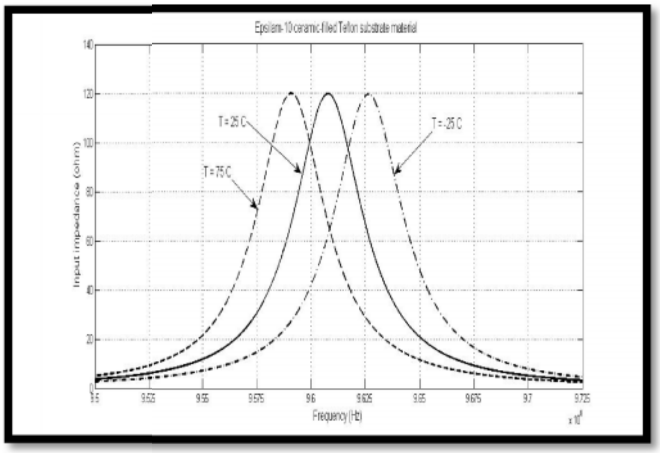

Figure. 25. Real part of the input impedance as a function of frequency at different temperatures 75, 25 and -25 ^{0}C and radius of curvature 50 mm.

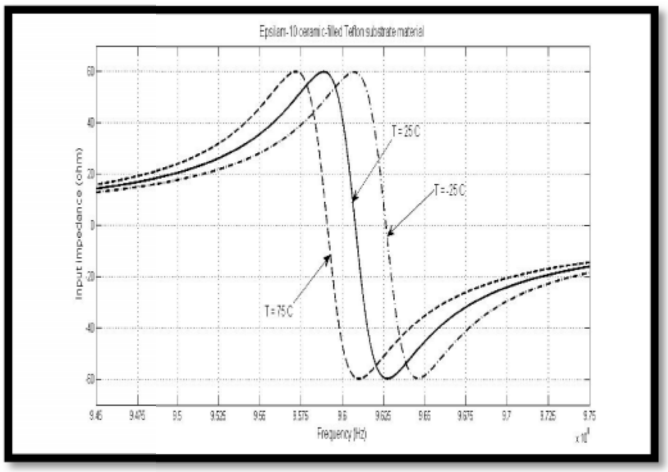

Figure. 26. Imaginary part of the input impedance as a function of frequency at different temperatures 75, 25 and -25 ^{0}C and radius of curvature 50 mm.

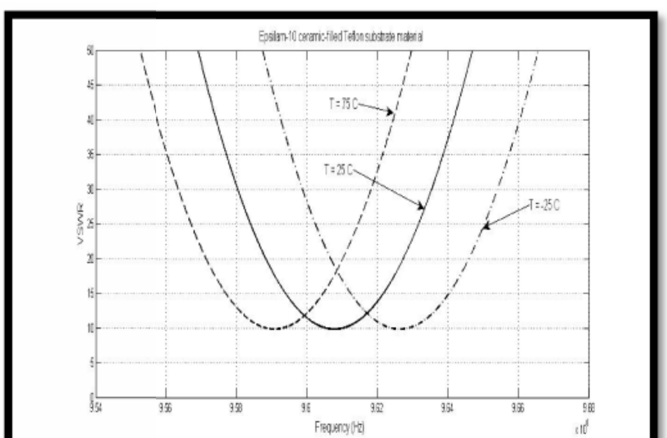

Figure. 27. VSWR versus frequency at different temperatures 75, 25 and -25 ^{0}C and radius of curvature 50 mm.

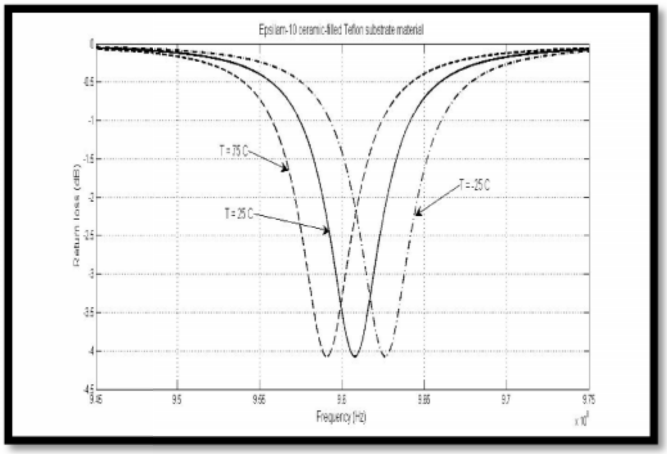

Figure. 28. Return loss (S11) as a function of frequency at different temperatures 75, 25 and -25 ^{0}C and radius of curvature 50 mm.

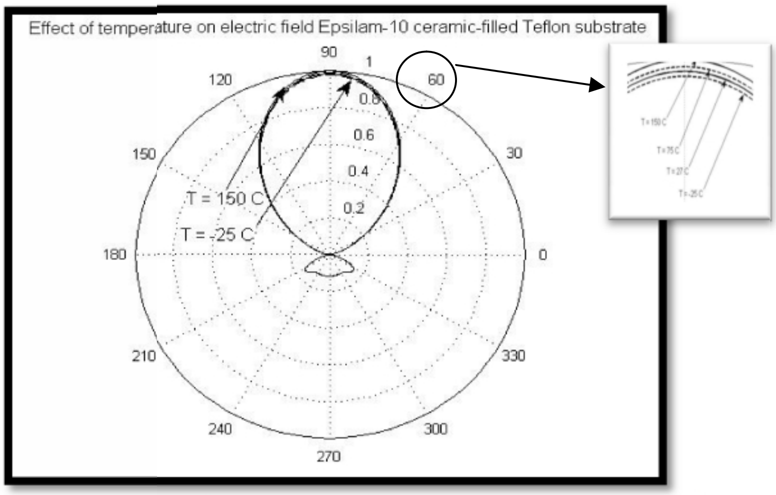

Figure. 29. Normalized electric field for different temperatures 150, 75, 27 and -25 ^{0}C. at θ=0:2π and $\varphi=0^0$ and radius of curvature 50 mm.

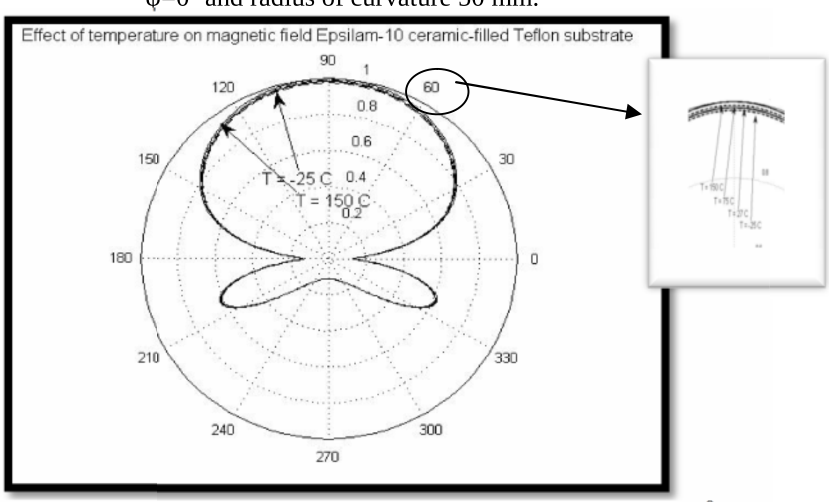

Figure. 30. Normalized magnetic field for different temperatures 150, 75, 27 and -25 ^{0}C. at θ=0:2π and $\varphi=0^0$ and radius of curvature 50 mm.

Conclusion

The effect of temperature on the performance of a conformal microstrip printed antenna used for a projectile flight on a high distance is very important to study. The temperature affects the three different substrates effective dielectric constant and hence affect the operating resonance frequency for TM_{01} mode. The effect of temperature on input impedance, VSWR and return loss are also studied for a radius of curvature of 50 mm. We notice that, as the temperature increases, the effective dielectric constant is also increases for different materials used. On the other hand, the resonance frequency decreases with increasing temperature. VSWR and return loss are decreasing as the temperature increases.

The change in resonance frequency is between 40 MHz for TM_{01} mode. This shift is very small for a wide range of temperature used, but it is very effective in case of using frequency hopping technique.

References

[1] Heckler, M.V., et al., CAD Package to Design Rectangular Probe-Fed Microstrip Antennas Conformed on Cylindrical Structures. roceedings of the 2003 SBMO/IEEE MTT-S International, Microwave and Optoelectronics Conference, 2003. , 2003. 2: p. 747-757.

[2] Q. Lu, X. Xu, and M. He, Application of Conformal FDTD Algorithm to Analysis of Conically Conformal Microstrip Antenna. IEEE International Conference on Microwave and Millimeter Wave Technology, ICMMT 2008. , April 2008. 2: p. 527 – 530.

[3] Wong, K.L., Design of Nonplanar Microstrip Antennas and Transmission Lines. 1999: John & Sons, Inc.

[4] Josefsson, L. and P. Persson, Conformal Array Antenna Theory and Design 1ed. 2006: Wiley-IEEE Press.

[5] Thomas, W., R.C. Hall, and D. I. Wu, Effects of curvature on the fabrication of wraparound antennas IEEE International Symposium on Antennas and Propagation Society,, 1997. 3: p. 1512-1515.

[6] J. Byun, B. Lee, and F.J. Harackiewicz, FDTD Analysis of Mutual Coupling between Microstrip Patch Antennas on Curved Surfaces. IEEE International Symposium on Antennas and Propagation Society, 1999. 2: p. 886-889.

[7] D. Schaubert, F. Farrar, A. Sindoris, and S. Hayes, “Microstrip antennas with frequency agility and polarization diversity,” IEEE Trans. on Antennas and Propag., vol. 29, no. 1, pp. 118-123, Jan. 1981.

[8] M. Richard, K. Bhasin, C. Gilbert, S. Metzler, G. Koepf, and P. Claspy, “Performance of a four-element Ka-band high-temperature superconducting microstrip antenna,” IEEE Microwave and Guided Wave Letters, vol. 2, no. 4, pp. 143 – 145, Apr. 1992.

[9] J. Huang, and A. Densmore, “Microstrip Yagi array antenna for mobile satellite vehicle application,” IEEE Trans. on Antennas and Propag., vol. 39, no. 7, pp. 1024 - 1030 , Jul. 1991.

[10] S. Jacobsen, and P. Stauffer, “Multifrequency radiometric determination of temperature profiles in a lossy homogeneous phantom using a dual-mode antenna with integral water bolus,” IEEE Trans. on Microwave Theory and Techniques, vol. 50, no. 7, pp. 1737 – 1746, Jul 2002.

[12] H. Kolodziej, D. Bem, and P. Kabacik, “Measured Electric Characteristics of Various Microwave Substrates,” COST 245 Action Active Phased Arrays Array-Fed Antennas-Eur. Union, Brussels, Belgium, 1995.

[13] Balanis, C.A., AntennaTheory. 2005, New York: John Wiley & Sons.

[14] Pozar, D., Microstrip Antennas. IEEE Antennas and Propagation Proceeding, 1992. 80(1).

[15] Krowne, C.M., Cylindrical-Rectangular Microstrip Antenna. IEEE Trans. on Antenna and Propagation, 1983. AP-31: p. 194-199.

[16] T. Seki, N. Honma, K. Nishikawa, and K. Tsunekawa, “High Efficiency Multi-Layer Parasitic Microstrip Array Antenna on TEFLON Substrate,” 34th European Microwave Conf. - Amsterdam, pp. 829-832, Oct. 2004.

[17] T. Seki, N. Honma, K. Nishikawa, and K. Tsunekawa, “Millimeter-Wave High Efficiency MultiLayer Parasitic Microstrip Antenna Array on TEFLON Substrate,” IEEE Trans. on Microwave Theory and Techniques, vol. 53, no. 6, pp. 2101-2106, Jun. 2005.

[18] P. Kabacik, and M. Bialkowski, “The Temperature Dependence of Substrate Parameters and Their Effect on Microstrip Antenna Performance,” IEEE Trans. on Antennas and Propag., vol. 47, no. 6, pp. 1042-1049, Jun. 1999.

[19] A. Hammoud, E. Baumann, I. Myers, and E. Overton, “Electrical Properties of Teflon and Ceramic Capacitors at High Temperatures,” IEEE International Symp. on Electrical Insulation, Baltimore, MD USA, pp. 487-490, Jun. 1992.

[20] F. Patrick , R. Grzybowski, and T. Podlesak , High-Temperature Electronics, CRC Press Inc., 1997.

[21] A. Hammoud, E. Baumann, I. Myers, and E. Overton, “High Temperature Properties of Apical, Kapton, PEEK, Teflon AF, and Upilex Polymers,” Annual Report Conf. on Electrical Insulation and Dielectric Phenomena, pp. 549-554, Aug. 2002.

[22] L. Ting,” Charging Temperature Effect for Corona Charged Teflon FEP Electrets,” 7th International Symp. on Electrets, pp. 287-292, Aug. 2002.

[23] S. Dhawan, “Understanding Effect of Teflon Room Temperature Phase Transition on Coax Cable Delay in Order to Improve the Measurement of TE Signals of Deuterated Polarized Targets,” IEEE Trans. on Nuclear Science, vol. 39,no. 5, Oct. 1992.

[24] P. Kabacik, and M. Bialkowski, “The Temperture Dependence of Substrate Parameters and Their Effect on Microstrip Antenna Performance,” IEEE Transaction on Antennas and Propagation, vol. 47, no. 6, June 1999.

[25] K. Carver, and J. Mink, “Microstrip Antenna Technology,” IEEE Transaction on Antennas and Propagation, vol. 29, no. 1, January 1981.

[26] L. W. Mckeen, The Effect of Temperature and Other Factors on Plastic and Elastomers, William Andrew, New York, 2007.

[27] A. Elrashidi , K. Elleithy, and Hassan Bajwa, “The Fringing Field and Resonance Frequency of Cylindrical Microstrip Printed Antenna as a Function of Curvature,” International Journal of Wireless Communications and Networking, July-Dec 2011, Accepted

BIBLIOGRAPHIES

Ali Elrshidi, Ali is Ph.D student in University of Bridgeport. Ali received the Bachelor in communication engineering from the University of Alexandria, Egypt 2002. He got his master degree in fiber optics field in 2006 from the same university under supervision of Prof: Ali Okaz, Prof. Moustafa Hussien, and Dr: Keshk. He works in a project funded by US Army, to control the motion of a small projectile using two small stepper motors. Also, Ali has designed a microstip printed antenna works at 2.4 GHz and gives a high performance.

Dr. Elleithy is the Associate Dean for Graduate Studies in the School of Engineering at the University of Bridgeport. He has research interests are in the areas of network security, mobile communications, and formal approaches for design and verification. He has published more than one hundred fifty research papers in international journals and conferences in his areas of expertise. Dr. Elleithy is the co-chair of the International Joint Conferences on Computer, Information, and Systems Sciences, and Engineering (CISSE). CISSE is the first Engineering/Computing and Systems Research E-Conference in the world to be completely conducted online in real-time via the internet and was successfully running for four years.Dr. Elleithy is the editor or co-editor of 10 books published by Springer for advances on Innovations and Advanced Techniques in Systems, Computing Sciences and Software.
Dr. Elleithy received the B.Sc. degree in computer science and automatic control from Alexandria University in 1983, the MS Degree in computer networks from the same university in 1986, and the MS and Ph.D. degrees in computer science from The Center for Advanced Computer Studies at the University of Louisiana at Lafayette in 1988 and 1990.

Hassan Bajwa, Ph.D., is an Assistant Professor of Electrical Engineering at The University of Bridgeport. He received his BSc degree in Electrical Engineering from Polytechnic University of New York in 1998. From 1998 to 2001 he worked for Software Spectrum and IT Factory Inc, NY. He received his MS from the City College of New York in 2003, and his Doctorate in Electrical Engineering from City University of New York in 2007. Dr. Hassan research interests include low power sensor networks, flexible electronics, RF circuit design, Antennas, reconfigurable architecture, bio-electronics, and low power implantable
implantable devices. He is also working on developing biomedical instruments and computation tools for bioinformatics.